Comparison of experimental and density functional study on the molecular structure, infrared and Raman spectra and vibrational assignments of 6-chloronicotinic acid

Mehmet Karabacak [a,*], Mustafa Kurt [b]

[a] Department of Physics, Afyon Kocatepe University,
TR-03040, Afyonkarahisar, Turkey
[b] Department of Physics, Ahi Evran University, TR-40100, Kırşehir, Turkey

Abstract

The experimental and theoretical study on the structures and vibrations of 6-chloronicotinic acid (6-CNA, $C_6H_4ClNO_2$) are presented. The Fourier transform infrared spectra (4000–50 cm^{-1}) and the Fourier transform Raman spectra (3500–50 cm^{-1}) of the title molecule in solid phase have been recorded, for the first time. The geometrical parameters and energies have been obtained for all four conformers from DFT (B3LYP) with different basis sets calculations. There are four conformers, C1, C2, C3, and C4 for this molecule. The computational results diagnose the most stable conformer of 6-CNA as the C1 form. The vibrations of the two stable and two unstable conformers of 6-CNA are researched with the aid of quantum chemical calculations. The molecular structure, vibrational frequencies, infrared intensities and Raman scattering activities and theoretical vibrational spectra were calculated a pair of molecules linked by the intermolecular O−H···O hydrogen bond. The spectroscopic and theoretical results are compared to the corresponding properties for 6-CNA stable monomers and dimer of C1 conformer.
© 2008 Published by Elsevier B.V.

Keywords: IR and Raman spectra; DFT; 6-chloronicotinic acid; Vibrational frequencies; Molecular structure

1. Introduction

Nicotinic acid and its derivatives, which have biological activities, have been studied extensively over the past decade. The structures of many of the complexes that have been reported show nicotinic acid and its derivatives acting as bridging ligands through the carboxylate group and pyridyl N atom [1]. The nicotinic acid and its complexes with different metals were thoroughly investigated different methods [2–3]. First time, the solid-state structure of nicotinic acid was determined in 1953 [4]. The biological and chemical importance of this type of compounds and especially its complexes are described in the literature [5–6].

Chloronicotinic acid is simple amphoteric electrolytes of considerable biological interest. Certain of its derivatives indicate remarkable physiological activity [7]. 6-Chloronicotinic acid (6-CNA) is important building blocks for agrochemicals, animal food enrichment, feed additives, reduce plasma cholesterol and pharmaceuticals [8].

Density functional theory (DFT) calculations are reported to provide excellent vibrational frequencies of organic compounds if the calculated frequencies are scaled to compensate for the approximate treatment of electron correlation [9–18]. The calculations based on DFT have been applied in many areas, and the results also are in great agreement with the experimental results in calculating vibrational frequencies [19–21].

Extensive experimental and theoretical investigations have focused on elucidating the structure and normal vibrations of nicotinic acid derivatives. Vibrational assignment based FT-IR and Raman spectra and theoretical DFT calculations have been studied for picolinic, nicotinic and isonicotinic acids [5]. Sala et al. [6] investigated vibrational modes of nicotinic acid by both experimental as well as theoretical methods, however, literature survey reveals that to the best of our knowledge, no experimental and computational vibrational spectroscopic study on free 6-CNA is published in the literature yet. This inadequacy observed in the literature encouraged us to make this theoretical and experimental vibrational spectroscopic research based on

---
* Corresponding author. Tel.: +90 272 2281311; fax: +90 272 2281235.
   E-mail address: karabacak@aku.edu.tr (M. Karabacak).

the conformers of molecule to give a correct assignment of the fundamental bands in experimental FT-IR and FT-Raman spectra. Therefore, present study aims to give a complete description of the molecular geometry and molecular vibrations of the 6-CNA. The possible stable conformers of 6-CNA molecule were searched. The optimized geometry of the conformers and vibrational frequencies for the two stable and other conformers of 6-CNA were calculated at DFT/B3LYP level of theory using the 6-311++G(d,p) basis set. C1 form is the more stable conformer than C2 stable conformer. The results of the theoretical and spectroscopic studies are reported herein. Also, the vibrational wavenumbers of 6-CNA dimer of C1 conformer have also been calculated. These calculations are valuable for providing insight into the vibrational spectrum and molecular parameters. A detailed interpretation of the vibrational spectra of 6CNA has been made on the basis of the calculated total energy distribution (TED).

2. Experimental

The compound 6-CNA sample was purchased from Acros Organics Company with a stated purity 99% and it was used as such without further purification. 6-CNA is in solid phase. Therefore, the FT-IR spectrum (4000–400 cm^{-1}) of KBr disc of the sample was recorded on a PerkinElmer FT-IR System Spec-

trum BX spectrometer and fewer 400 cm^{-1} on a Bruker IFS 66/S which were calibrated using polystyrene bands. FT-Raman spectra of the sample was recorded using 1064 nm line of Nd:YAG laser as excitation wave length in the region 50–3500 cm^{-1} on a Bruker FRA 106/S FT-Raman. The detector is a liquid nitrogen cooled Ge detector.

3. Computational details

The geometry data was taken from X-ray structure [22]. In order to obtain stable structures, the geometrical parameters for four conformers and dimer of 6-CNA in the ground state (in vacuo) were optimized at DFT by the B3LYP level of theory using the 6-311G(d), 6-311G(d,p), and 6-311++G(d,p) basis sets. Moreover, the vibrational wavenumbers of 6-CNA dimer with H-bonding between carboxyl groups of C1 conformation have also been calculated to improve simulation of the experimental spectra. The vibrational frequencies for the four conformers are calculated with this method and then wavenumbers in the ranges from 4000 to 1700 cm^{-1} and lower than 1700 cm^{-1} are scaled with 0.958 and 0.983, respectively [18]. We tabulated only C1 conformer calculations data because of most stable conformer. All the calculations are performed by using Gaussview molecular visualisation program [23] and Gaussian 03 program package on the personal computer [24].
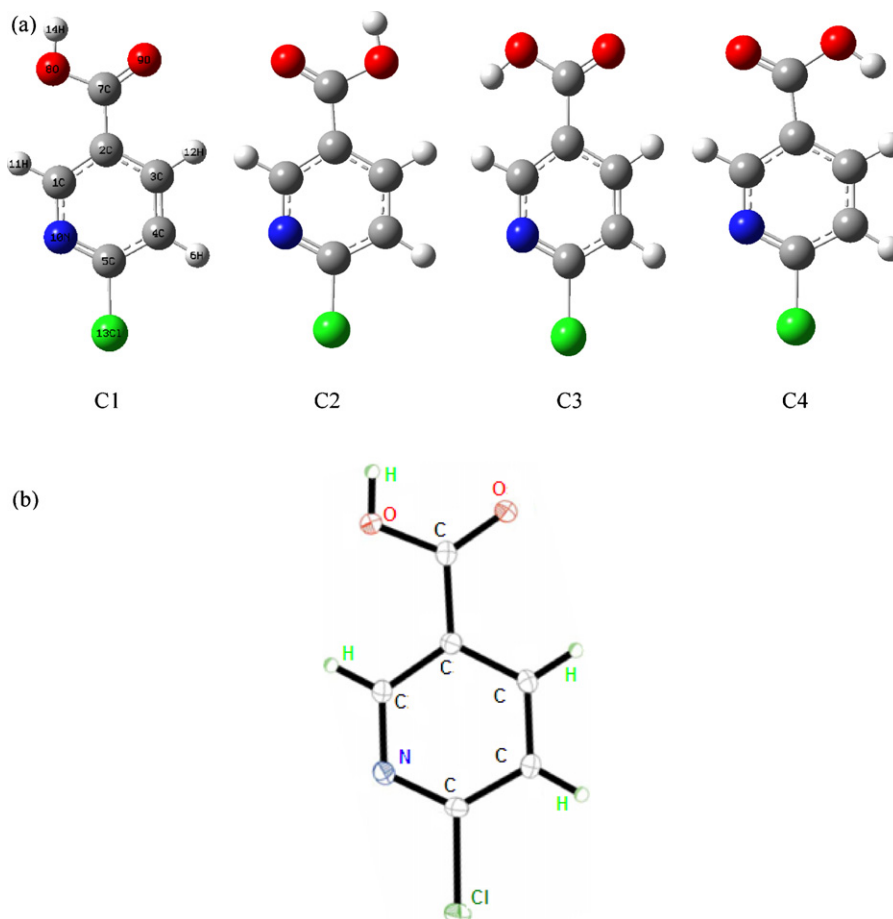

Fig. 1. (a) The theoretical geometric structures and atomic numbering scheme of 6-CNA (all conformers). (b) The experimental geometric structure of 6-CNA with displacement ellipsoids drawn 50% probability level (arbitrary spheres for the H atoms) taken from Ref. [22].

The Becke's three-parameter hybrid density functional, B3LYP [25,26], was used to calculate harmonic vibrational wavenumbers with the 6-311++G(d,p) basis set. It is well known in the quantum chemical literature that among available functional the B3LYP functional yields a good description of harmonic vibrational wavenumbers for small and medium sized molecules.

4. Results and discussion

In the C1, C2, C3, and C4 forms of molecule, nicotinic acid and pyridine ring are in the same plane. The molecular structures and numbering of the atoms of 6-CNA and C1 dimer form of 6-CNA are shown in Figs. 1 and 2, respectively. We reported some geometric parameters and vibrational frequencies for 6-CNA by using DFT (B3LYP) and compared with the experimental crystal geometries (bond lengths, bond angles) [22] and experimental frequencies.

4.1. Energetics

Calculated energies and energy difference for all conformers of 6-CNA molecule, determined by B3LYP level 6-311G(d), 6-311G(d,p), and 6-311++G(d,p) are presented in Table 1. From DFT calculations with 6-311++G(d,p) basis set, the conformer C1 is predicted to be from 0.268 to 8.648 kcal/mol more stable the other conformers. Additionally, because of the imaginary frequency, the calculations showed the conformers C3 and C4 to be unstable conformer. As clearly seen from the values given in Table 1, the basis set size effect on the calculated energies is not so much, but of considerable importance; use of the basis sets of larger sizes give rise to slight increases in the differences between the calculated energies of the stable conformers, however, unstable conformers give rise to decreases in the differences between the calculated energies.

4.2. Geometrical structures

The molecular structure of 6-CNA has been studied by X-ray diffraction [22]. According to the result of X-ray analysis [22], the crystals belong to the triclinic system, with the space group $P\bar{1}$ and the cell dimensions $a = 3.741$ (1) Å, $b = 5.761$ (1) Å, $c = 14.737$ (4) Å, $V = 309.23$ (13) Å^3 and $z = 2$. The first task for the computational work was to determine the optimized geometry of 6-CNA. The atomic numbering schemes of all conformers (C1, C2, C3, and C4) of 6-CNA are shown in Fig. 1. Intermolecular hydrogen bonds can be responsible for the geometry and the stability of a predominant conformation; the formation of hydrogen bonding between a hydroxyl group and O=COH cause the structure of the conformer C1 to be the most stable conformer.

The predicted bond lengths and bond angles for two conformers of 6-CNA and dimer of C1 conformer of 6-CNA are tabulated in Table 2 in comparison to the experimental values obtained from 6-CNA crystal [22]. Taking into account that the molecular geometry in the vapour phase may be different from in the solid phase, owing to extended hydrogen bonding and stacking interactions there is reasonable agreement between the calculated and experimental geometric parameters. Compari-
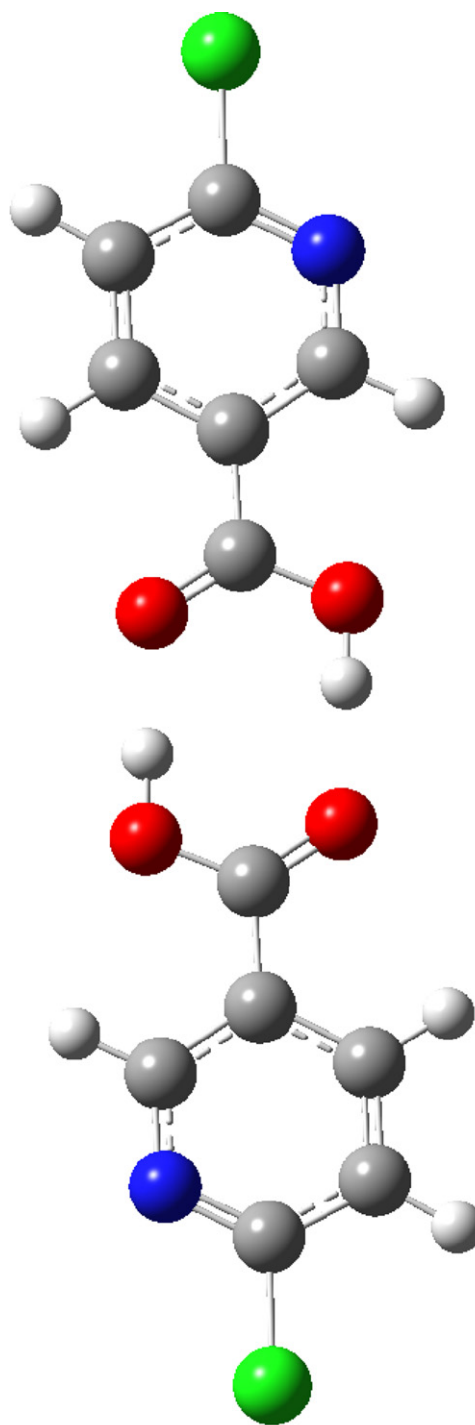

Fig. 2. The theoretical geometric structure of dimer C1 conformer of 6-CNA.

son of the calculated and observed bond lengths, the theoretical parameters are bigger than experimental data.

As discussed by Johnson et al. [27], DFT method predicts bond lengths which are systematically too long, particularly the C–H bond lengths. This theoretical pattern also found for 6-CNA. Since the large deviation from experimental C–H bond lengths may arise from the low scattering of hydrogen atoms in the X-ray diffraction experiment. The perceivable ones are for the bond distances of C–H among which the biggest difference is

Table 1
Calculated energies and energy difference for four conformers of 6-CNA by DFT method

Conformers	B3LYP 6-311G(d)		B3LYP 6-311G(d,p)		B3LYP6-311 + +G(d,p)	
	Energy (hartree)	Energy differences[a] (kcal/mol)	Energy (hartree)	Energy differences[a] (kcal/mol)	Energy (hartree)	Energy differences[a] (kcal/mol)
C1	−896.58917666	0.000	−896.60014719	0.000	−896.61170409	0.000
C2	−896.58881757	0.225	−896.59974914	0.250	−896.61127695	0.268
C3	−896.57556637	8.541	−896.58758620	7.882	−896.59959292	7.600
C4	−896.57382938	9.631	−896.58596441	8.900	−896.59792188	8.648

[a] Energies of the other three conformers relative to the most stable C1 conformer.

Table 2
Comparison of geometric parameters, bond length (Å), and bond angle (°), for the monomer and dimer C1 conformer of 6-CNA calculated by the B3LYP 6-311 + +G(d,p) method

Parameters	X-ray[a]	C1	Dimer (C1)
Bond lengths (Å)			
C(1)−C(2)	1.393	1.397	1.397
C(1)−N(10)	1.338	1.337	1.336
C(1)−H(11)	0.950	1.083	1.084
C(2)−C(3)	1.397	1.400	1.400
C(2)−C(7)	1.480	1.485	1.483
C(3)−C(4)	1.379	1.384	1.384
C(3)−H(12)	0.950	1.083	1.083
C(4)−C(5)	1.394	1.398	1.398
C(4)−H(6)	0.950	1.081	1.081
C(5)−N(10)	1.322	1.318	1.318
C(5)−Cl(13)	1.738	1.756	1.755
C(7)−O(8)	1.318	1.354	1.320
C(7)−O(9)	1.226	1.208	1.229
O(8)−H(14)	0.840	0.969	1.000
H⋯A	1.800		1.666
D⋯A	2.638		2.665
σ (rms)		0.071	0.078
Bond angles (°)			
C(2)−C(1)−N(10)	123.2	123.0	123.0
C(2)−C(1)−H(11)	118.4	120.7	120.5
N(10)−C(1)−H(11)	118.4	116.3	116.4
C(1)−C(2)−C(3)	118.5	118.1	118.2
C(1)−C(2)−C(7)	121.4	122.8	122.1
C(3)−C(2)−C(7)	120	119.0	119.7
C(2)−C(3)−C(4)	118.9	119.2	119.2
C(2)−C(3)−H(12)	120.5	119.4	119.5
C(4)−C(3)−H(12)	120.5	121.3	121.3
C(3)−C(4)−C(5)	117.2	117.2	117.2
C(3)−C(4)−H(6)	121.4	122.0	122.0
C(5)−C(4)−H(6)	121.4	120.8	120.8
C(4)−C(5)−N(10)	125.4	124.8	124.9
C(4)−C(5)−Cl(13)	118.9	118.6	118.6
N(10)−C(5)−Cl(13)	115.6	116.6	116.6
C(2)−C(7)−O(8)	113.8	112.8	114.3
C(2)−C(7)−O(9)	122.3	124.6	121.8
O(8)−C(7)−O(9)	123.9	122.6	123.8
C(7)−O(8)−H(14)	109.5	107.2	110.4
C(1)−N(10)−C(5)	116.6	117.5	117.5
D-H⋯A	176		178.9
σ (rms)		1.241	1.057

[a] The X ray data from Ref. [22].

0.134 Å. These bond lengths were found to be 0.95 Å in 6-CNA crystal [22], but theoretically calculated data are bigger than 1 Å. Other perceivable one is for bond distance C−Cl among which is approximately 0.02 Å bigger than experimental value (1.738 Å) which is in good agreement with calculated value. Bakiler et al. calculated this bond length 1.746 Å for 3-chloropyridine [28] and 1.748 Å for 2-chloropyridine [29] by using force field calculations. These bond lengths were also observed 1.735–1.744 Å range for similar molecules [30,31]. The structural parameters are found to be similar for two stable conformers (C1 and C2). Most of the bond angles and distances are almost the same but there are some differences that should be mentioned. However, there are small differences other conformations that should be touched on. This one is C−O bonds which C1 conformer's data are approximate the experimental data. C1 conformer has the shortest $C_7−O_8$ bond distance by 1.354 Å, this band obtained 1.318 Å with X-ray [22]. There is the shortest $O_8−H_{14}$ bond distance in C4 conformer by 0. 963 Å, however this band obtained 0.840 Å [22]. The bond distance $C_2−C_7$ among in C1 and C2 conformers is bigger (0.017 Å) than C3 and C4 conformers. This bond was found to be 1.480 Å in 6-CNA crystal [22] and calculated as the biggest in unstable conformers (C3 and C4, 1.501 Å) probably due to effect of hydrogen on the structure.

In the ring part optimized geometry of the molecule shows very good agreement with experiment. For example, the calculated $C_2=C_3$ bond length, 1.400 Å (C1 and C2) reproduces the measured bond length within the experimental accuracy, 1.397 Å. Other bond length (C=N) in the ring that is calculated 1.337 Å and measured 1.338 Å. The similar correlation was found for pyridine [32], methyl pyridine [33].

The CCC and CNC angles are calculated 117–119° ranges which are smaller hexagonal angle of 120° for studied molecule. But CCN angle found to be bigger than ca. 4° hexagonal angles for C1 conformation. Similar values found to be other pyridine derivatives [30,31,34]. The largest difference for the angles comes from $\angle C_2C_7O_8$ in the C2 conformer which is less by ca. 5° than that of the C3 conformer. However, $\angle C_2C_7O_9$ angle in the C2 conformer which is more 3° than that of the C3 conformer. The dihedral angles are nearly the same among the all conformers. The remaining angles are nearly the same among the all conformers except for the angle $C_7O_8H_{14}$.

To make comparison with experimental data, we present rms (σ) values based on the calculations bottom of Table 2. The rms for bond lengths and bond angles values are 0.071 and 1.241
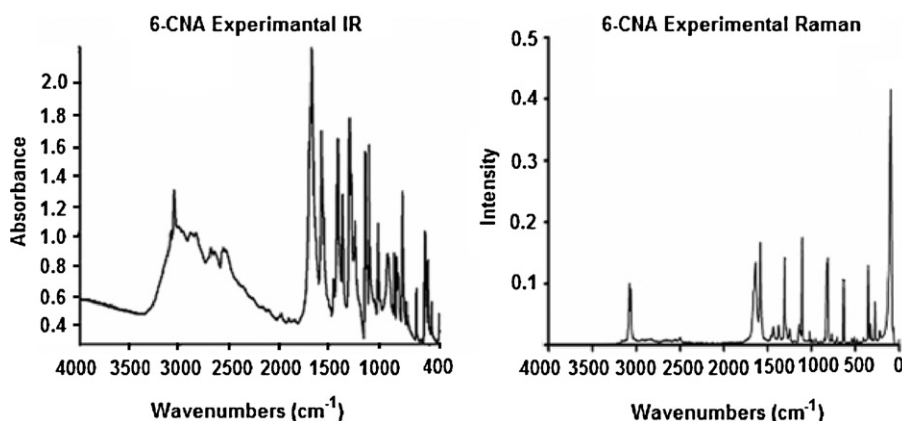
Fig. 3. The experimental FT-IR and FT-Raman spectrum of 6-CNA molecule.

for C1 conformer. The plots linear with a unit slope and the correlation (R^2) values are found to be 0.9731 and 0.9116 for bond lengths and bond angles for C1 conformation.

4.3. Vibrational spectra

The present molecule 6-CNA consists of 14 atoms, so it has 36 normal vibrational modes. On the basis of a C_s symmetry the 36 fundamental vibrations four forms of title molecule can be distributed as $25A' + 11A''$. The vibrations of the A' species are in plane and those of the A'' species are out of plane. All vibrations are active in both IR and Raman. But if the molecules were C_1 symmetry there would not be any relevant distribution. Calculations were made for a free molecule in vacuum, while experiments were performed for solid samples, so there are disagreements between calculated and observed vibrational wavenumbers.

Fig. 3 presents the experimental FT-IR and FT-Raman spectra of 6-CNA, respectively. The experimental wavenumbers are tabulated in Table 3 together with the calculated wavenumbers for monomer and dimer C1 conformer of studied molecule. The resulting vibrational frequencies for the optimized geometries and the proposed vibrational assignments as well as IR intensities and Raman scattering activities are given in Table 3. In the last column is given a detailed description of the normal modes based on the total energy distribution. The symmetry species of all the vibrations are written in the first column of the table. Modes are numbered from biggest to smallest frequency within each fundamental wavenumbers, ν. Some vibration bands found in the predicted IR spectra were not observed in the experimental spectrum of 6-CNA. For example, hydrogen bonding in the condensed phase with the other acid molecules makes vibrational spectra more complicated. Therefore, we could not observe the sharp and strong bands of O–H vibration in the Raman and IR spectra. To the best of our knowledge there is no vibrational data for gas phase 6-CNA. Therefore, we have to compare calculated results with those of solid phase vibrational spectrum. In order to simulate H bonding through COOH group we also calculate vibrational wavenumbers of 6-CNA dimer of C1 conformer (see Table 3).

Owing to lack of enough detailed experimental data for this molecule, the vibrational spectrum was obtained by molecular orbital calculation using Gaussian 03 [24] program. Vibrational modes of 6-CNA were researched by harmonic frequency calculations performed at the corresponding energy optimized geometries. The assignment of the vibrational absorptions was made by the comparison with the related molecule and also with the results obtained from the theoretical calculations [5,6,21,35]. The descriptions of the modes presented here are only approximate, being some of the vibration mixed together.

For 6-CNA, group the vibrational modes are CH stretching modes, CO stretching modes, CCl stretching modes, CN stretching modes, CC stretching modes, OH stretching modes, CCH bending, CCC bending, CCN bending, OCO bending, ring bending and ring torsion. In the spectral range over 3000 cm^{-1}, O–H and C–H stretching modes take place. In the range of 1800–1500 cm^{-1}, the C–C, C=O and COOH group stretching vibrations occur. Two of mixed modes involving contributions from C–C stretching as well as O–H in plane deformations and CN stretching are observed in the 1500–1350 cm^{-1} range. Between 1350–400 cm^{-1} several characteristic in plane deformations C–H, out-of-plane C–H vibrations as well as out-of-plane (CCC) deformations observe [5].

The heteroaromatic structure shows the presence of C–H stretching vibrations in the 3000–3100 cm^{-1} range which is the characteristic region for the ready identification of C–H stretching vibrations [36,37]. Accordingly, in the present study, the three adjacent hydrogen atoms left around the ring the 6-CNA give rise three C–H stretching modes ($\nu2$–$\nu4$), three C–H in plane bending ($\nu11$, $\nu12$, $\nu14$) and three C–H out-of-plane bending ($\nu18$, $\nu19$, $\nu20$) vibrations which corresponds to stretching modes of C_1–H_{11}, C_3–H_{12}, C_4–H_6 units. The vibrations $\nu2$–$\nu4$ assigned to aromatic C–H stretching in the region 3066–3144 cm^{-1} [21] are in agreement with experimental assignment 3058–3092 cm^{-1} [37]. These modes are calculated from 3081 to 3063 cm^{-1} for the most stable C1 conformer. In the IR spectrum, C–H peaks were observed in the 3042–3104 cm^{-1} range for nicotinic acid by Koczon et al. [5]. In aromatic compounds, C–H in plane bending frequencies appear in the range of 1000–1300 cm^{-1} and C–H out-of-plane bending vibration in the range 750–1000 cm^{-1}

Table 3
Comparison of the experimental (FT-IR and FT-Raman) wavenumbers (cm^{-1}) and theoretical harmonic frequencies (cm^{-1}), infrared intensities (I^{Infrared} (km mol^{-1})), Raman scattering activities (Å^{-4} amu^{-1}) of C1 monomer and dimer conformers of 6-CNA calculated by the B3LYP method using 6-311 + +G(d,p) basis set

Mode no.	Symmetry species	Experimental		Theoretical C1 monomer conformer				Theoretical C1 monomer conformer		
		FT-IR	FT-Raman	Unscaled frequency	Scaled frequency[a]	I^{Infrared}	S^{Raman}	Unscaled frequency	Scaled frequency[a]	TED[b] (%)
ν1	A′			3769	3610	117.7	146.9	3204, 3110	3069, 2979	νOH (100)
ν2	A′	3092 vw	3077 m	3216	3081	0.5	122.3	3218, 3218	3083, 3083	νCH (99)
ν3	A′		3062 m	3198	3063	1.0	48.5	3200, 3200	3066, 3066	νCH (100)
ν4	A′	3058 m		3197	3063	1.6	68.6	3197, 3197	3063, 3063	νCH (98)
ν5	A′	1681 s	1644 m	1791	1716	418.7	134.5	1736, 1690	1663, 1661	νCO (85)
ν6	A′	1582 vs	1584 m	1624	1597	186.5	127.9	1625, 1624	1597, 1596	νCC (47) ring + νCN (19) + δCCH (16)
ν7	A′			1594	1567	24.9	1.9	1593, 1592	1566, 1565	νCC (63) ring + νCN (14) + δCCH (7)
ν8	A′	1463 vw 1420 s		1492	1467	50.6	4.2	1497, 1497	1472, 1472	δCCH (53) + νCC (20) ring + νCN (15)
ν9	A′	1374 m	1376 vw	1395	1371	89.8	6.9	1395, 1394	1371, 1370	δCCH (37) + νCC (23) ring + νCN (21) + δCCC (4)
ν10	A′	1301 s	1308 m	1370	1347	147.7	19.8	1475, 1452	1450, 1427	δOH (29) + δCO (22) + νCC (17) + δCH (10)
ν11	A′	1286 w		1314	1292	4.3	2.7	1313, 1313	1291, 1291	δCH (60) + νCN (27)
ν12	A′	1248 w	1258 vw	1299	1277	2.8	2.7	1292, 1290	1270, 1268	νCC (50) ring + νCN (39) + νCC (12) + δOH (7)
ν13	A′			1207	1187	159.3	40.3	1333, 1327	1310, 1304	δOH (46) + νC-COOH (16) + δCH (10)
ν14	A′	1143 s	1141 vw	1153	1133	12.2	0.8	1153, 1153	1133, 1133	δCH (60) + νCC (22) ring + νCCl (5)
ν15	A′	1107 s	1108 m	1119	1100	293.0	38.2	1119	1100	νCN (23) + δCH (20) + νCC (13) + νCCl (11) + νC-OH (8)
ν16	A′	1053 vw		1112	1093	106.1	4.9	1118	1099	Ring breathing (50) + νC-OH (43) + δCOH (4)
ν17	A′	1018 m	1019 vw	1035	1018	14.2	1.0	1036, 1036	1018, 1018	δCCH (25) + δCCC (20) + νCC (17) + δCNC (12) + νCN (9)
ν18	A″	993 vw		1007	990	0.4	0.0	1006, 1006	989, 989	γC-H (89)
ν19	A″	918 m		970	954	2.6	0.5	974	957	γC-H (84) + τCCCN (5)
ν20	A″	851 m 830 m	826 m	859	845	9.9	0.3	860, 860	845, 845	γC-H (80) + τCCCO (9)
ν21	A′	815 vw		812	799	43.0	24.4	834, 828	820, 814	δCCC (30) + δCCN (19) + νC-COOH (13) + νC-Cl (9)
ν22	A″	771 s	774 vw	783	770	54.0	0.2	783, 780	770, 767	τCCCH bend (40) + τCCCO (32) + τOCOH (17)
ν23	A″	728 vw		734	722	13.0	0.0	729, 727	717, 715	τCCNC (41) + τCCCH (14) + τC-COOH (14) + τCCCC (10)
ν24	A′			684	672	16.0	0.7	736, 719	724, 707	δOCO (28) + δCCO (15) + νCCl (10) + δCCC (8)
ν25	A′	634 w	637 m	641	630	1.7	6.4	642, 642	631, 631	i.p. Pyridine Ring deformation (85)
ν26	A′	546 m	546 vw	579	569	77.4	2.7	976, 972	959, 956	γOH (85)
ν27	A′	519 m	519 vw	522	513	24.8	0.9	550, 537	541, 528	νCCl (27) + δCCO (26) + δOCO (9) + δCCC (7) + δClCN (5)
ν28	A″	482 vw		493	484	42.5	0.5	519, 509	510, 500	δC-OH (40) + νCCl (18) + δOCO (14) + δCCC (5)
ν29	A″			481	473	22.7	0.5	491, 490	483, 482	τCCCN (30) + τCCCH (21) + τCCCC (13) + τCCCO (12) + γOH (9)
ν30	A′	406 vw		418	411	5.2	0.2	417, 416	410, 409	τCCCN (32) + τCCCC (28) + τCCCH (20)
ν31	A″		354 m	328	323	0.4	1.6	351, 325	345, 320	δCCl (52) + δCCO (13) + νCCl (8) + δCCC (6)
ν32	A′	312 w	325 vw	309	304	1.3	4.1	357, 312	351, 307	δCCl (17) + δCCC (16) + νCCl (15) + νC-COOH (14) + δCNC (13)
ν33	A″		279 w	253	249	0.2	0.5	270, 265	265, 261	ω Pyridine Ring (78) + τCOOH (5)
ν34	A′			170	167	2.2	0.5	227, 220	223, 216	δC-COOH (57) + δCCO(19) + δCCl (17)
ν35	A″		97 vs	83	81	0.2	0.1	111, 88	109, 87	ω6CNA (93)
ν36	A″		65 vw	66	65	3.3	0.3	62	61	τCCCO (98)
σ (rms)				51.154	20.883					

[a] Wavenumbers in the ranges from 4000 to 1700 cm^{-1} and lower than 1700 cm^{-1} are scaled with 0.958 and 0.983, respectively.
[b] Total energy distribution, ν; stretching, δ; in-plane bending, γ; out-of-plane (o.o.p.) bending, ω; wagging, τ; torsion, vs; very strong, s; strong, m; medium, w; weak, vw; very weak.

[38]. The CH in plane bends are assigned to the FT-IR bands at 1286, 1248 and 1143 cm^{-1}, respectively. The CH out-of-plane bends are assigned to the FT-IR bands in the range from 993 to 830 cm^{-1}. Both the in-plane and out-of-plane bending vibrations are described as mixed modes. The ring breathing mode ($\nu16$) is predicted at 1093, 1086, 1079, and 1073 cm^{-1} all conformers, respectively, which is observed at 1053 cm^{-1} in the FT-IR spectrum. The theoretically calculated C—C—C in-plane and out-of-plane bending modes have been obtained to be consistent with the recorded spectral values.

Empirical assignments of vibrational modes for peaks in the fingerprint region are difficult. In the wavenumber region of 600–1660 cm^{-1}, the spectrum observed in the experiments closely resembles the calculated spectrum, except for differences in details.

The C—N stretching frequency is a rather difficult task since there are problems in identifying these frequencies from other vibrations. Sundaraganesan [21] assigned C—N stretching absorption in the region 1381 cm^{-1} for 2-amino-5-iodopyridine. In the present work, the band observed at 1374 cm^{-1} in FT-IR spectrum (1376 cm^{-1} in FT-Raman) has been assigned to C—N stretching vibration. The theoretically computed value C—N stretching vibration (1371 cm^{-1} for C1 conformer) is in excellent agreement with experimental observation. The theoretically computed value of C—N stretching vibration may be probably mixing other vibrations.

The most characteristic feature of carboxylic group is a single band observed usually in the 1700–1800 cm^{-1} region. This band is due to the C=O stretching vibration. In the solid state most of carboxylic acids form a dimeric structure that is due to the result of hydrogen bonding between two neighbouring –COOH groups. In such a case two ν(C=O) are expected: one that is Raman active (in–phase, symmetric stretching vibration) and the other one, out-of-phase (antisymmetric stretching vibration), is IR active only. The asymmetric stretch is usually at higher wavenumber than the symmetric stretch. Therefore, the C=O stretching mode ($\nu5$, asymmetric stretching vibration) is observed at 1681 cm^{-1} in the FT-IR spectrum and observed at 1644 cm^{-1} (symmetric stretching vibration) in the FT-Raman spectrum which is predicted at 1716 cm^{-1} (C1) and 1719 cm^{-1} (C2). The hydrogen bonding effect through the carboxyl groups, therefore C1 dimer conformation C=O stretching mode calculated at 1663 and 1661 cm^{-1}. This mode however, is predicted at 1740 cm^{-1} for C3 and 1742 cm^{-1} for C4 conformer. In previous paper [39], we assigned as 1721 cm^{-1} FT-IR (1712 cm^{-1} FT-Raman) C=O stretching vibration. C=O stretching mode is observed at 1725 cm^{-1} Raman spectra by Sala et al. [6]. Koczon et al. [5] in the IR spectra, observed C=O stretching mode at 1717 cm^{-1} for picolinic acid, 1708 cm^{-1} nicotinic acid and 1712 cm^{-1} for isonicotinic acid. It means that presence of nitrogen in aromatic ring and its position versus carboxylic acid influence the mode form very slightly, but in the experimental spectra the shift of various bands along with the change of nitrogen position is remarkable. By the chlorine substitution in place of hydrogen atom, the chlorine position versus carboxylic anion influence the C=O mode form remarkably.

The ring stretching vibrations are very much important in the spectrum of pyridine and its derivatives are highly characteristic of the aromatic ring itself. The ring carbon–carbon stretching vibrations occur in the region 1430–1625 cm^{-1}. In the present work, the C=C stretching modes are expected and the highest one is observed at 1582 cm^{-1} ($\nu6$) in the FT-IR spectrum and 1584 cm^{-1} in the FT-Raman.

The OH vibrations in carboxylic acids are extremely sensitive to formation of hydrogen bonding. O—H stretching band is characterized by very broadband appearing near about 3400–3600 cm^{-1}. This band calculated 3610 cm^{-1}, however, it is not observed experimentally. The O—H in plane bending vibration occurs in the general of 1440–1395 cm^{-1} [40]. In 6-CNA, the O—H in plane bending is assigned to 1301 cm^{-1} FT-IR and 1308 cm^{-1} FT-Raman. The O—H out of plane bending is observed at 546 cm^{-1} in the FT-Raman. Theoretically computed values (1347 and 569 cm^{-1}) are in very good agreement with experimental results. The O—H in plane bending and out of plane bending vibrations values in dimer conformations are increasing, because of the hydrogen bonding effect through the carboxyl groups (see Table 3).

Some vibrational modes were shown to be Cl–sensitive modes whereas others were calculated in a narrow frequency range. The theoretical wavenumbers of C—Cl stretching vibration coupled with other group vibrations. The bending modes were located at 280–300 cm^{-1} range for chloro derivates. The calculated bending mode is approximately 323, 304, and 167 cm^{-1} for C1 form. The C—Cl stretching modes are 600–800 cm^{-1} frequency range. Our calculations show that there are in the 480–800 cm^{-1} range C—Cl stretching bands. In the earlier vibrational studies of 3-chloro-2-, 2-chloro-6-, 4-chloro-2-, and 5-chloro-2-methyl anilines are observed 650–670 cm^{-1} the υ(C—Cl) bands [30,41,42]. The remainder of the observed and calculated frequencies accounted in Table 3.

The infrared intensity for title molecule from experimental fundamentals ($\nu6$) at 1582 cm^{-1} is very strong, theoretical intensity (all conformation) of these fundamentals is not in the same order. This may be attributed to the inadequacy of the DFT methods as the basis set in predicting the intensities of the A′ frequencies of the molecule. While experimental intensity is very strong for this mode, calculated intensity is 186.5 km mol^{-1} for C1 conformer. This mode corresponds to CC stretching mode. The most calculated intensity is 418.7 km mol^{-1} which corresponds to CO stretching mode. The most Raman scattering activity (146.9 Å^{-4}amu^{-1}) peak is calculated corresponds to the O—H stretching mode.

In general, our infrared intensities and Raman scattering activities are very high when compared with those at the lower frequency region (Table 3). While experimental and calculated high intensities may lead to the true identification in the assignments of fundamentals, theoretical and experimental low intensities may lead to the wrong identification in the assignment of fundamentals [33], especially in the lowest frequency region. As known previously, because of reasons, such as anharmonic effect, vibrational intensity could not be estimated very accurately using quantum chemistry software till now.

To make comparison with experimental data, we present rms (σ) values based on the calculations bottom of Table 3. The rms error of the frequencies between the unscaled and experimentally observed was found to be 51.154 and after scaling, the rms error between the observed and scaled frequencies of the molecule was found to be 20.883 cm^{-1} for C1 conformation. The plots are linear with a unit slope and the correlation values are found to be 0.9990 and 0.9991 for unscaled and scaled frequencies for C1 conformation.

The calculated wavenumbers for dimer 6-CNA shown in Fig. 2 are tabulated in Table 3. As seen in Table 3, the hydrogen bonding effect through the carboxyl groups is clearly observed (e.g. in ν1, ν5, ν10, ν21, and ν26 modes). This is agreement with Akkaya and Akyüz [19].

5. Conclusions

In this work, we have performed the experimental and theoretical vibrational analysis of 6-CNA, for the first time. A comparison of the result of experimental and theoretical study gave us a full description of the geometry and vibrational properties of this molecule. Based on calculated energy differences, the C1 conformer is found to be most the stable conformer and C3 and C4 conformers are predicted the unstable conformer. Intermolecular hydrogen bonding between H and O is expected in C1 conformer. In C1 conformer, C=O stretching (ν8) wavenumber found to be lower than the other conformers and C1 conformer has the longest C7O9 bond distance. Dimeric molecules held together by hydrogen bridges between carboxyl groups. The calculated geometric parameters and vibrational frequencies obtained with density functional theory calculations (B3LYP/6-311 + +G(d,p)) method are in good agreement with the experimental values obtained for the investigated molecule.

References

[1] S. Gao, J. Liu, L. Huo, Z. Sun, J. Gao, S. Weng Ng, Acta Cryst. (2004) m363–m365.
[2] C.L. Broadhurst, W.F. Schmidt, J.B. Reeves, M.M. Polansky, K. Gautschi, et al., J. Inorg. Biochem. 66 (1997) 119.
[3] N.K. Singh, D.K. Singh, et al., Synth. React. Inorg. Met. -Org. Chem. 32 (2002) 203.
[4] W.B. Wright, G.S.D. King, Acta Cryst. 6 (1953) 305–317.
[5] P. Koczon, J.Cz. Dobrowolski, W. Lewandowski, A.P. Mazurek, J. Mol. Struct. 655 (2003) 89–95.
[6] O. Sala, N.S. Gonçalves, L.K. Noda, J. Mol. Struct. 565–566 (2001) 411–416.
[7] S.K. Dogra, J. Luminescence 114 (2005) 213–226.
[8] W.C.J. Ross, Biochem. Pharmacol. 16 (1967) 675–680.
[9] D. Michalska, W. Zierkiewicz, D.C. Bieńko, W. Wojciechowski, Th. Zeegers-Huyskens, J. Phys. Chem. A 105 (2001) 8734; W. Zierkiewicz, D. Michalska, Th. Zeegers-Huyskens, J. Phys. Chem. A 104 (2000) 11685.
[10] P.M. Wojciechowski, W. Zierkiewicz, D. Michalska, P. Hobza, J. Chem. Phys. 118 (2003) 10900.
[11] D. Michalska, R. Wysokiński, Chem. Phys. Lett. 403 (2005) 211–217.
[12] M. Kurt, J. Mol. Struct. 874 (2008) 159.
[13] N.C. Handy, C.W. Murray, R.D. Amos, J. Phys. Chem. 97 (1993) 4392.
[14] P.J. Stephens, F.J. Devlin, C.F. Chavalowski, M.J. Frisch, J. Phys. Chem. 98 (1994) 11623.
[15] F.J. Devlin, J.W. Finley, P.J. Stephens, M.J. Frish, J. Phys. Chem. 99 (1995) 16883.
[16] S.Y. Lee, B.H. Boo, Bull. Korean Chem. Soc. 17 (1996) 754.
[17] G. Rauhut, P. Pulay, J. Phys. Chem. 99 (1995) 3093.
[18] N. Sundaraganesan, S. Ilakiamani, H. Saleem, P.M. Wojciechowski, D. Michalska, Spectrochim. Acta A 61 (2005) 2995.
[19] Y. Akkaya, S. Akyüz, Vibrational Spectrosc. 42 (2006) 292–301.
[20] Ş. Yurdakul, M. Yurdakul, J. Mol. Struct. 834–836 (2007) 555–560.
[21] N. Sundaraganesan, C. Meganathan, B. Ananda, B. Dominic Joshua, Christine Lapouge, Spectrochim. Acta Part A 67 (2007) 830–836.
[22] S. Long, M. Siegler, T. Li, Acta Cryst. E63 (2007) o279–o281.
[23] P.L. Fast, J. Corchado, M.L. Sanches, D.G. Truhlar, J. Phys. Chem. A 103 (1999) 3139.
[24] M.J. Frisch, et al., Gaussian 03, Revision B. 4, Gaussian Inc., Pittsburgh PA, 2003.
[25] A.D. Becke, J. Chem. Phys. 98 (1993) 5648.
[26] C. Lee, W. Yang, R.G. Parr, Phys. Rev. B 37 (1988) 785.
[27] B.G. Johnson, P.M. Gill, J.A. Pople, J. Chem. Phys. 98 (1993) 5612.
[28] M. Bakiler, I.V. Maslov, S. Akyüz, J. Mol. Struct. 482–483 (1998) 379.
[29] M. Bakiler, I.V. Maslov, S. Akyüz, J. Mol. Struct. 475 (1999) 83.
[30] M. Kurt, M. Yurdakul, Ş. Yurdakul, J. Mol. Struct. 711 (2004) 25–32.
[31] A.K. Rai, S. Kumar, A. Rai, Vibrational Spectrosc. 42 (2006) 397.
[32] J.O. Jensen, Vibrational Spectrosc. 30 (2002) 191.
[33] J.E. del Bene, J. Am. Chem. Soc. 101 (1979) 6184.
[34] A.E. Ozel, S. Kecel, S. Akyüz, Vibrational Spectrosc. 42 (2006) 325.
[35] Scot H. Brewer, A.M. Allen, S.E. Lappi, T.L. Chase, K.A. Briggman, C.B. Gorman, S. Franzen, Langmuir 20 (2004) 5512–5520.
[36] V. Krishnakumar, R. Ramasamy, Spectrochim. Acta Part A 62 (2005) 570–577.
[37] M. Silverstein, G. Clayton Basseler, C. Morill, Spectrometric Identification of Organic Compounds, Wiley, New York, 1981.
[38] N. Sundaraganesan, S. Ilakiamani, B.D. Joshua, Spectrochimica Acta Part A 67 (2007) 287–297.
[39] M. Karabacak, M. Çınar, M. Kurt, Journal of Molecular Structure 885 (2008) 28–35.
[40] N. Sundaraganesan, B.D. Joshua, K. Settu, Spectrochim. Acta A 66 (2007) 381.
[41] L. Santos, E. Martinez, B. Ballesteros, J. Sanchez, Spectrochim, Acta Part A 56 (2000) 1905.
[42] J. Hanuza, M. Maczka, A. Waslowska, W. Oganowski, M. Andruszkiewicz, H.B. Ogonowska, B. Lutz, V. der-Maas, J. Mol. Struct. 404 (1997) 33.